

Qubit Lattice Algorithm for Two-Dimensional Electromagnetic Scattering from Scalar Dielectric Objects

George Vahala¹, Min Soe², Linda Vahala³, Abhay K. Ram⁴

¹*William & Mary, Williamsburg, U.S.A*

²*Rogers State University, Claremore, U.S.A*

³*Old Dominion University, Norfolk, U.S.A*

⁴*M. I. T, Cambridge, U.S.A*

There is considerable interest in applying quantum information science to problems in plasma physics, even though most magnetic fusion plasmas are well into the classical regime. In some sense, this is a natural outcome building on the efforts [1], [2] in the 1930's of connecting Maxwell equations in a vacuum with the Dirac equation for a massless free particle. From the unitary qubit lattice algorithm (QLA) of Yezpez [3] for the Dirac equation, we [4], [5] extended [3] to handle electromagnetic pulse propagation in inhomogeneous refractive media. QLA consists of an interleaved sequence of non-commuting unitary collision-streaming operators acting on a basis set of qubits which in the continuum limit recover the continuum system of interest perturbatively. Some potential operators are also introduced to incorporate the non-derivative terms and one or more of these operators are Hermitian (and not unitary).

In particular, we [6] have shown through both 1D QLA simulations and electromagnetic theory that the reflection and transmission of a pulse incident normally onto a (continuous) dielectric boundary agrees with the standard boundary value plane wave Fresnel conditions except that our initial value problem will have a transmitted electric field amplitude that is augmented over the Fresnel amplitude by the factor $\sqrt{n_2/n_1}$ of the two media refractive indices.

Here we present some QLA simulations for the scattering of a 1D electromagnetic pulse off an isolated scalar dielectric object, with refractive index $n = n(x, z)$. The full Maxwell equations can be represented by an 8-spinor wavefunction [7]. The qubit basis set is just that derived from the Riemann-Silberstein-Weber vectors [7], \mathbf{F}^\pm :

$$\Psi^\pm = \begin{pmatrix} -F_x^\pm \pm iF_y^\pm \\ F_z^\pm \\ F_z^\pm \\ F_x^\pm \pm iF_y^\pm \end{pmatrix}, \quad \text{with} \quad \mathbf{F}^\pm = n(\mathbf{x})\mathbf{E} \pm \mathbf{i} \frac{\mathbf{B}}{\sqrt{\mu_0}}. \quad (1)$$

For pulse propagation in the x-direction, the time evolution of the qubit equation is determined just from this 8-qubit representation since the collision operator must entangle different

qubit basis elements. However, in z-propagation we run into the problem that the time and spatial derivative of the qubits couple the same qubit elements. Thus, to devise a unitary collision operator we must double the number of qubits to finish with a 16-qubits QLA [5].

We first consider the scattering of a 1D electromagnetic pulse, propagating in the x-direction, as it interacts with a localized dielectric cylinder, Fig. 1. During the propagation in the vacuum ($n_1 = 1$), the only non-zero field components are $E_y(x, t)$ and $B_z(x, t)$

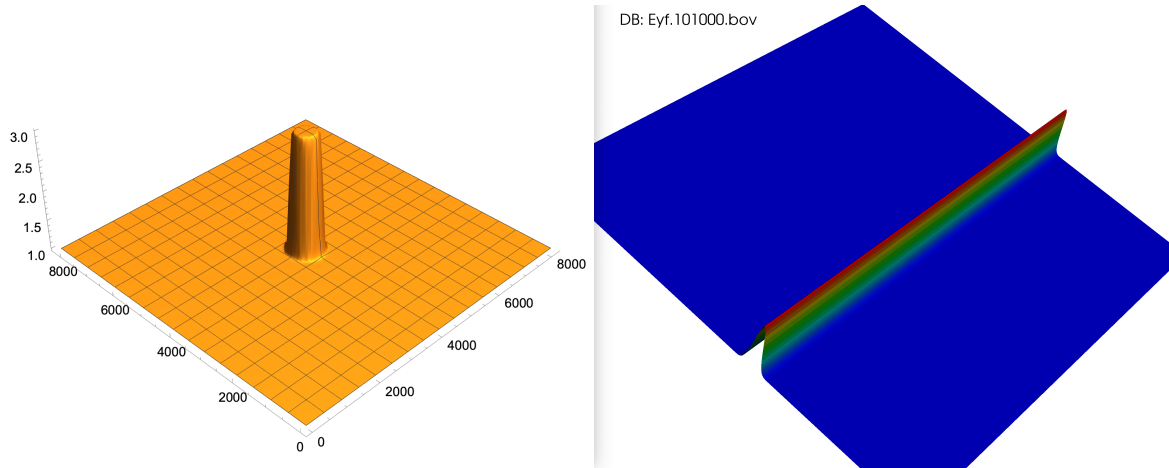


Figure 1: (a) the dielectric cylinder $n(x, z)$, (b) The E_y of the initial electromagnetic pulse .

As the 1D pulse interacts with the 2D dielectric cylinder of higher refractive index, the immediate reflected ring of E_y is negative, as seen in Fig. 2a, echoing the typical 1D Fresnel jump conditions for plane waves. The 2D nature of the scattering leads to the outgoing reflected circular pulse propagating back into medium n_1 .

As the 1D pulse scatters and penetrates the 2D dielectric, the symmetry breaking will generate a $B_x(x, z, t)$ field so that $\nabla \cdot \mathbf{B} = 0$. A snapshot of this B_x -field is shown in Fig. 2b. Away from the dielectric cylinder the pulse retains its speed and structure. In this region no symmetry breaking occurs and automatically $\nabla \cdot B_z(x, t)\hat{y} = 0$ without the need of generating a B_x component. Fig. 2b shows the self-consistently generated B_x field, showing the dipole structure quite clearly in the outer wavefront ring.

The later stages of the E_y field are shown in Fig. 3. The somewhat complex wavefronts are due to internal reflections of the incident pulse within the dielectric cylinder, followed by transmission/re-radiation of the pulse out into region n_1 .

In Fig 4 we consider a smaller width initial pulse now propagating towards a conic dielectric scatterer which peaks at $n_{2, max} = 3$ but has gentler variations in $n(x, z)$ in both x and z. Because the slopes are very weak at the base of the dielectric cone, there is very little reflection in E_y from

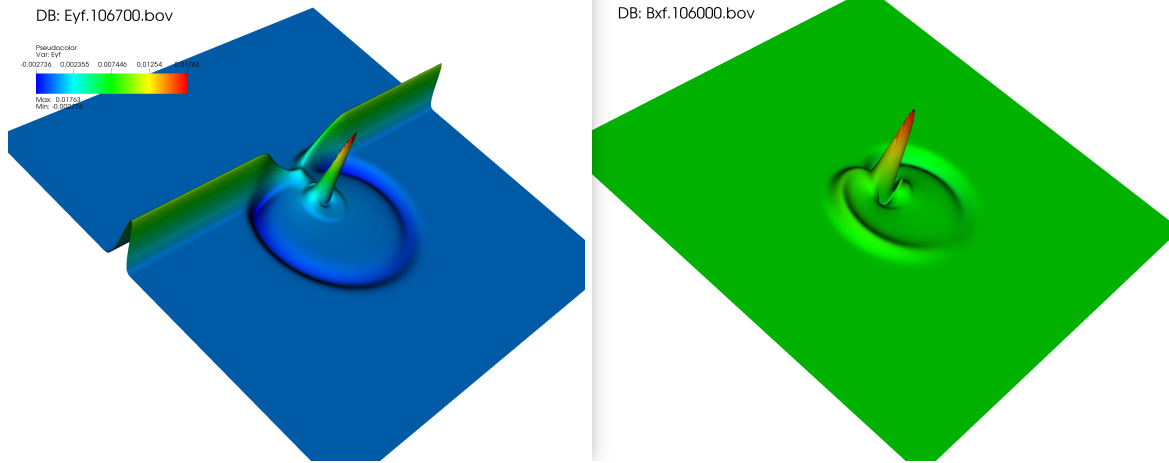


Figure 2: (a) Early stage of scattering of E_y , (b) The generation of B_x field

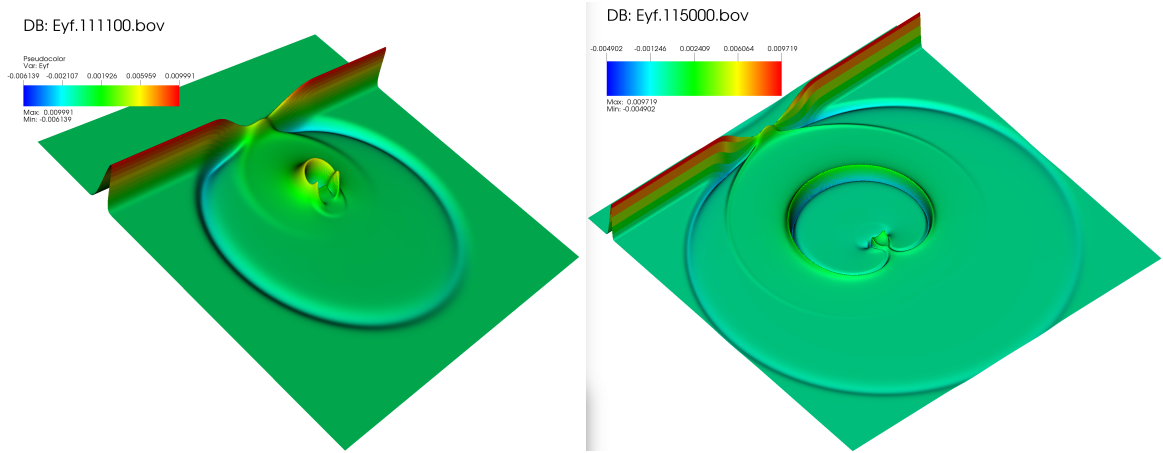


Figure 3: (a) Later stages of scattering of E_y , (b) The $E_y(x,z,t)$ at the end of the QLA simulation.

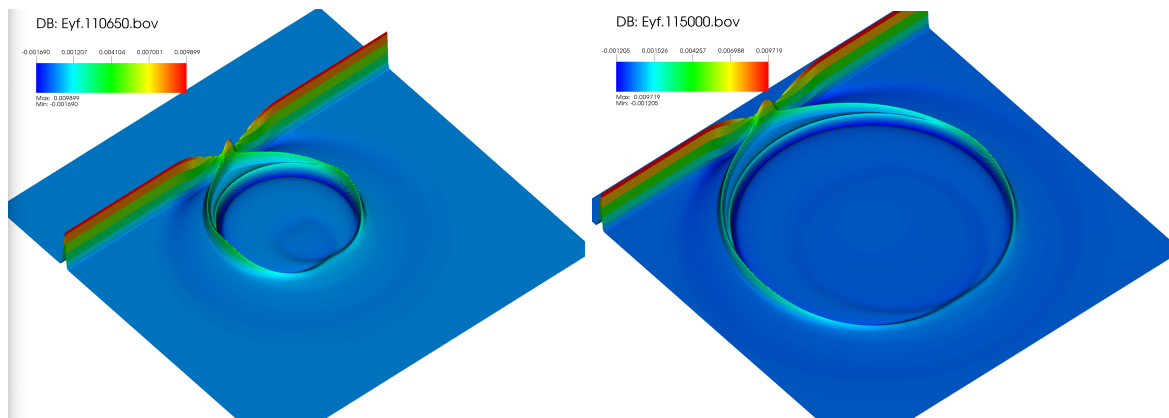


Figure 4: (a) Early stage of scattering of E_y , (b) The $E_y(x,z,t)$ at the end of the QLA simulation.

this region. On comparing with a similar evolution time for scattering from a dielectric cylinder, Fig. 3a, there is no outer ring of substantial $E_y < 0$ in Fig. 4a. As the pulse moves closer to the apex of the cone, the refractive index gradients are considerably steeper resulting in a reflected circular pulse. On comparing Fig. 4b with Fig. 3b we see negligible internal bouncing of the pulse within the dielectric cone. For the dielectric cylinder one still finds sloshing within the dielectric along with the accompanying emitted wave fronts.

Finally we comment on the perturbative parameter introduced in QLA. Because the 2D QLA consists of 16 interleaved unitary collision/streaming operators their explicit evaluation in Mathematica requires the introduction of a perturbation parameter ε into the collision angles in order to complete the required algebra. In the continuum limit we recover the full Maxwell equations to $O(\varepsilon^2)$. In our earlier QLA for the nonlinear Schrodinger equation (NLS), this ε was related to the amplitude of the wave function. Here, in Maxwell equations, it is found from simulations that ε is related directly to the speed of pulse propagation in medium 1. For NLS there was a window $[\varepsilon_L, \varepsilon_U]$ in which QLA very accurately recovered all the soliton-soliton collision of the exactly soluble NLS [8]. However from the QLA simulations for Maxwell equations we recover the correct electromagnetic scattering behavior for arbitrary ε within the window $[0.01, 1.00]$, where the limit $\varepsilon = 1$ is the maximum permitted value for CFL number for numerical stability.

Future work will be to generalize the QLA to handle tensor dielectric media and the cold plasma dispersion relation.

Acknowledgments

This research was partially supported by Department of Energy grants DE-SC0021647, DE-FG02-91ER-54109, DE-SC0021651, DE-SC0021857, and DE-SC0021653. The simulations were performed on CORI of the National Energy Research Scientific Computing Center (NERSC), A U.S. Department of Energy Office of Science User Facility located at Lawrence Berkeley National Laboratory, operated under Contract No. DE-AC02-05CH11231.

References

- [1] A. O. Laporte and E. G. Uhlenbeck, Phys. Rev. **37**, 1380 (1931)
- [2] J. R. Oppenheimer, Phys. Rev. **38**, 725 (1931)
- [3] J. Yepez, Quant. Info. Proc. **5**, 471 (2005)
- [4] G. Vahala, L. Vahala, M. Soe and A. K. Ram, J. Plasma Phys **86**, 905860518 (2020)
- [5] G. Vahala, L. Vahala, M. Soe and A. K. Ram, Rad Effects Defects in Solids **176**, 49, 64 (2021)
- [6] A. K. Ram, G. Vahala, L. Vahala, and M. Soe, AIP Advances **11**, 105116 (2021)
- [7] S. A. Khan, Physica Scripta **71**, 440 (2005)
- [8] G. Vahala, L. Vahala, and J. Yepez, Phys. Lett A **310**, 187 (2003)